Dependence of beating dynamics on the ellipticity of a Gaussian beam in graded-index absorbing nonlinear fibers

D. Ianetz,[1] Yu. Kaganovskii,[1] and A. D. Wilson-Gordon[2]

[1]*The Jack and Pearl Resnick Institute for Advanced Technology, Department of Physics, Bar-Ilan University, Ramat-Gan 52900, Israel*

[2]*Department of Chemistry, Bar-Ilan University, Ramat Gan 52900, Israel*

(Received 18 March 2013; published 26 April 2013)

Using the collective variable approach technique, we analyze propagation of elliptical Gaussian beams in nonlinear waveguides with a parabolic graded-index (GRIN) profile. We considered both saturable and cubic-quintic models to describe the nonlinearity, taking into account both linear and nonlinear absorption. For lossless media, we construct diagrams, which define regions of self-focusing and self-diffractive beam propagation for both models in GRIN waveguides and compare them with those for nongraded waveguides. The widths of the propagating elliptic beam exhibit an oscillatory pattern, similar to the "breathing" and "beating" behavior found in nongraded media. Two types of beating oscillations are observed in both models. We calculate the dependence of $L_{\mathrm{beat}}/L_{\mathrm{br}}$, the ratio of the "beating" to "breathing" oscillation periods, on the beam ellipticity ρ and the GRIN index g. We find that there is a remarkable difference in this dependence between saturable and cubic-quintic media: in the saturable model, $L_{\mathrm{beat}}/L_{\mathrm{br}}$ is a monotonic function of ρ, whereas in the cubic-quintic model, it is characterized by singularities, which correspond to transitions between the types of beat oscillations. For lossy media, we discuss the difference between the breathing behavior in nongraded and GRIN waveguides.

DOI: 10.1103/PhysRevA.87.043839 PACS number(s): 42.65.Wi, 42.65.Jx, 42.65.Tg

I. INTRODUCTION

The propagation of a laser beam in a nonlinear fiber is the focus of many theoretical and experimental investigations [1–3] because of possible applications in optical communication technology and signal processing [4,5]. Optical sensors using optical fibers are increasingly being applied to the monitoring of acoustic waves, pressure, and magnetic and electric fields. Recently, there have been several attempts to incorporate nonlinear effects in fiber-optical sensing [6–8]. As is well known, the performance of photonic devices strongly depends on the refractive indices of the constituent materials, hence the recent surge of interest in using new Kerr media for ultrafast optical switching [9]. For typical fiber materials, the Kerr coefficient is of the order 5×10^{-15}–$5\times10^{-16}\mathrm{cm}^2/\mathrm{W}$, and thus the critical intensity for self-focusing is of the order $0.44-4.4\ \mathrm{MW/cm}^2$ for a wavelength of 1.5 μm [10]. In contrast, some new optical materials are characterized by Kerr coefficients of the order 10^{-11}–$10^{-12}\mathrm{cm}^2/\mathrm{W}$ [11–13], making the critical intensity for self-focusing four orders of magnitude smaller so that it can be reached using microsecond pulses and possibly even CW laser beams. The (linear and nonlinear) absorption coefficients of these materials are higher compared to those of typical fibers, and the propagation of laser beams through such media is of great interest. In this paper, we will discuss the propagation of elliptical Gaussian laser beams in nonlinear fibers, which are characterized by a graded-index (GRIN) refractive index and absorption.

In GRIN fibers, the refractive index n is high at the center and gradually decreases towards the cladding. It can be written in the form

$$n^2=\begin{cases}n_0^2-\mathrm{Gr}^2 & r<r_0\\ n_1^2 & r>r_0.\end{cases}\qquad(1)$$

Here, n_0 is the refractive index at the center of the waveguide $r=0$, $G>0$ is the graded-index constant, and n_1 is the refractive index of the cladding. If the beam is confined to a region in which $\mathrm{Gr}^2\ll n_0^2$ and the width of the propagating laser beam a is small compared to r_0, Eq. (1) becomes valid for all values of r. This is often referred to as the infinite-medium approximation [14,15]. The use of graded-index linear waveguides, in which the refractive index variation is of the form given by Eq.(1), avoids scattering on surface imperfections at the waveguide edges ($r=r_0$).

Although the GRIN fibers are mainly multimode, their refractive index profile generates differences in the average group velocities for the various modes. An axial mode propagating at small angles relative to the optical axis mostly experiences a high refractive index. Higher-order modes, propagating at larger angles relative to the axis, propagate close to the fiber cladding for a significant portion of their path and thus experience a lower refractive index. The differences in propagation speed compensate for the phase differences due to different propagation distances. With suitable index profiles the phase difference between the modes can be completely eliminated [5].

For a *linear lossless medium* in a parabolic GRIN waveguide, it has been shown analytically [14,15] that a cylindrical Gaussian beam with initial waist $a\ll r_0$ propagating along the axis of the graded-index waveguide remains Gaussian while its width oscillates (breathes) at a frequency that depends on $\sqrt{G}$. This occurs due to competition between the beam diffraction and focusing caused by GRIN. If the beam axis and the origin of the index profile are not aligned, the beam width oscillates around the index origin at a walk-off frequency that also depends on $\sqrt{G}$. When $\mathrm{Gr}^2\ll n_0^2$, all the propagating modes have the same group velocity [14,15]. Elliptical Gaussian beam propagates in the linear medium with the same breathing and walk-off frequencies as a cylindrical beam [14].

The propagation of cylindrical and elliptical Gaussian beam has also been analyzed for GRIN fibers consisting of a Kerr medium. The analysis was performed both numerically

and semianalytically. Numerical solutions [16] obtained for relatively low-intensity cylindrical Gaussian beams aligned along the fiber axis have displayed breathing of the waist. It was also shown that the fundamental nonlinear mode was stable; however, for higher-order modes, symmetry-breaking instabilities were observed.

Semianalytical solutions [17–26] for Kerr GRIN fibers have also shown that propagating beams of sufficiently low intensities exhibit breathing and walk-off behavior, as in a linear medium [14,15,27]. However, at higher intensities where the Kerr effect leads to self-focusing, collapse of the beam takes place [17,20,22,23]. Similar results were obtained for the propagation of elliptic Gaussian beams (EGBs). The power at which collapse occurs increased with the initial ellipticity of the incident EGB [19,21,24,28]. Recently, it was shown that beam collapse in Kerr media can be prevented by nonlocality of the material [29], whereas the power threshold for collapse can be altered by introducing partial coherence of the beam [30], or temperature fluctuations [31]. The conditions for collapse prevention in nonlinear media, for different dimensions of the nonlinear Schrödinger equation (NLSE), were defined in Refs. [1,32,33]. Thus, it seems that beam collapse in real materials can be prevented by nonlinearities of higher order (compared to the Kerr nonlinearity), due to their defocusing effect at high intensities.

It is worth noting that the problem of collapse and how to prevent it appears in the field of Bose-Einstein condensation (BEC), which is described by the same NLSE. In trapped BEC, it is well known that collapse occurs when the two-body interaction is attractive and if the number of atoms N exceeds a critical value N_c [34], so that the overall sign of the effective many-body interaction is negative. The nonlinear terms present in the NLSE (cubic, quintic, and so on) define the stability of the BEC when the number of atoms is restricted [35].

Here, we take these higher-order nonlinearities into account, and consider two models for GRIN fibers: the saturable model and the cubic-quintic (CQ) model. We study the effect of the beam ellipticity on the propagation dynamics for both these models and show striking differences between them.

First, for simplicity, we analyze the propagation of cylindrical Gaussian beams in lossless media. For this case, we construct diagrams, which define various regions of the beam behavior in both nongraded and GRIN waveguides for the saturable and cubic-quintic models. The diagrams define the regions of self-diffractive and self-focusing types of breathing in both media as a function of the GRIN constant. Moreover, for the cubic-quintic model, we find analytical solutions for the breathing period L_{br}, and for the beam waist a during the propagation, which can be expressed in terms of elliptic functions.

Second, we study elliptical Gaussian beams in lossless media, distinguishing between the oscillation of the beam about the fiber axis that occurs when the beam axis is displaced from the fiber axis (displacement frequency) and the oscillations of the beam widths caused by the beam ellipticity (beat frequency). We compare the propagation in GRIN waveguides with that in nongraded nonlinear media, which we have previously described [36–39] for both saturable and cubic-quintic models, taking into account both linear and nonlinear absorption. In our previous work, we identified two types of beats caused by the ellipticity: Type 1, in which the orientation of the major and minor axes of the elliptic beam remains constant during propagation, and Type 2, in which the major and minor axes interchange on propagation.

Here, we study the dependence of the beat dynamics on the beam ellipticity and show how the ratio of the beating to breathing periods varies with the ellipticity and the GRIN constant. We find remarkable differences between the saturable and cubic-quintic models. In the saturable model, the ratio is a monotonic function of the ellipticity, whereas in the cubic-quintic model, its behavior as a function of the ellipticity is characterized by singularities, which correspond to transitions between the types of beat oscillations. With increasing GRIN index, these singularities move to higher ellipticity.

Finally, we analyze the propagation of an elliptic beam behavior in lossy, saturable, and cubic-quintic media, and compare its behavior in GRIN waveguides with that in nongraded waveguides.

II. MODELS AND COLLECTIVE-VARIABLE APPROACH

We consider two different models of the media: the saturable and cubic-quintic models. In the saturable model, the nonlinear refractive index n in a GRIN waveguide can be expressed as

$$n^2 = n_0^2 + \frac{n_0\alpha_1|E|^2}{1 + n_0\alpha_1|E|^2/\left(n_{\mathrm{sat}}^2 - n_0^2\right)} - G(x^2 + y^2), \quad (2)$$

where n_0 is the linear refractive index, α_1 is the nonlinear Kerr coefficient, n_{sat} is the saturated index, and E is the envelope of the electric field.

In the cubic-quintic model, the refractive index of graded waveguides can be written in the form

$$n^2 = n_0^2 + n_0\alpha_1|E|^2 - n_0\alpha_2|E|^4 - G(x^2 + y^2). \quad (3)$$

In both cases we assume that the GRIN constant G does not depend on the light intensity and that the nonlinear coefficients are nongraded in the finite-medium approximation.

Equation (3) can be obtained from the Taylor expansion of Eq. (2) at low intensities with $\alpha_2 = \alpha_1^2 n_0/(n_{\mathrm{sat}}^2 - n_0^2)$. Both α_1 and α_2 are positive, and this form of nonlinearity describes competition between self-focusing at low intensities and self-defocusing at high intensities. However, it is worth noting that, in general, the cubic-quintic model cannot be considered as a special case of the saturable model [1,40], which is characterized by cubic and quintic terms of the same order of magnitude in the generalized nonlinear Schrödinger equation (GNLSE). As here we consider rather long laser pulses or CW beams, we can neglect the dispersion terms in our models [1,2,14,15].

For saturable media, the GNLSE that governs the evolution of the electric field of the beam in the slowly varying envelope approximation is given by

$$2i\beta\frac{\partial E}{\partial z} + \nabla_\perp^2 E + \frac{k_0^2 n_0\alpha_1|E|^2 E}{1 + (\alpha k_0 w_0)^2 n_0\alpha_1|E|^2} - k_0^2 G(x^2+y^2)E = -2i\beta\Gamma E - 2i\beta\Theta|E|^2 E, \quad (4)$$

where $\alpha = (k_0 w_0 \sqrt{n_{\rm sat}^2 - n_0^2})^{-1}$ is the saturation constant, k_0 and β are the wave numbers in the vacuum and medium, x, y, and z are the transverse and longitudinal coordinates, w_0 is a transverse scaling parameter related to the input beam width, and Γ and Θ are the linear and nonlinear absorption coefficients. Introducing the diffraction length $L_D = \beta w_0^2$, the normalized nonlinear amplitude $\psi = \sqrt{k_0 L_D \alpha_1} E$, and the normalized coordinates $x, y = \eta_{1,2} w_0$, $z = \zeta L_D$, $g = k_0^2 G w_0^4$, $\gamma = \beta \Gamma w_0^2$, and $\kappa = \Theta (k_0 \alpha_1)^{-1}$ [1], we can rewrite Eq. (4) in the form

$$2i\frac{\partial \psi}{\partial \zeta} + \frac{\partial^2 \psi}{\partial \eta_1^2} + \frac{\partial^2 \psi}{\partial \eta_2^2} + \frac{|\psi|^2 \psi}{1+\alpha^2|\psi|^2} - g\left(\eta_1^2 + \eta_2^2\right)\psi = -2i\gamma\psi - 2i\kappa|\psi|^2\psi. \quad (5)$$

The term $\nabla_\perp^2 \psi$ describes diffraction and the terms $|\psi|^2\psi/(1+\alpha^2|\psi|^2)$ and $g\eta_{1,2}^2\psi$ describe self-trapping in the transverse directions.

For the cubic-quintic model with the same normalized parameters and $Q = n_0 \alpha_2 (\alpha_1^2 \beta^2 w_0^2)^{-1}$, the GNLSE equation is written as

$$2i\frac{\partial \psi}{\partial \zeta} + \frac{\partial^2 \psi}{\partial \eta_1^2} + \frac{\partial^2 \psi}{\partial \eta_2^2} + |\psi|^2\psi - Q|\psi|^4\psi - g\left(\eta_1^2 + \eta_2^2\right)\psi = -2i\gamma\psi - 2i\kappa|\psi|^2\psi, \quad (6)$$

where the diffractive terms are $\nabla_\perp^2\psi$ and $Q|\psi|^4\psi$, and the terms $|\psi|^2\psi$ and $g\eta_{1,2}^2\psi$ describe self-trapping.

Due to the absence of exact analytical solutions of the GNLSE, approximate techniques can applied to Eq. (5) in order to find spatially localized solutions that preserve their shape during propagation. Although numerical solutions are preferable, they encounter difficulties caused by dependence of the speed and accuracy on the number and form of the nonlinear terms included in the GNLSE [2]. Careful selection of the step sizes in the propagation coordinates is required in order to achieve the necessary accuracy. Additional difficulties appear due to monotonic increase of the parabolic term with the radial distance. These can pose serious convergence problems for beam propagation algorithms [21]. The advantage of using explicit analytical or semianalytical solutions rather than numerical methods is that they give an overall picture of the behavior of the system thereby enabling increased physical insight [1,2].

To solve Eqs. (5) and (6) we use the collective variable approach (CVA), introduced by Anderson [41,42]. The CVA technique is based on a trial function—a simple analytical function whose amplitude and phase are as close as possible to the real solution. In our case, this is a Gaussian function with a finite number of variables, which are functions of the propagation coordinate that evolves subject to the constraints of the system. This choice is convenient because the Gaussian is the exact solution of the linear Schrödinger equation for GRIN waveguides.

Details of the method were previously described [43–46]. We first rewrite Eqs. (5) and (6) in the form $\hat{F}[\psi] = F_{\rm NC}$ where $\hat{F}[\psi]$, the conservative part, is expressed by the left-hand side (lhs) of Eqs. (5) and (6), and $F_{\rm NC}$, the nonconservative part, by the right-hand side (rhs) of the equation. We then define a Lagrangian density $\mathcal{L}[\psi, \psi^*]$ such that $\delta\mathcal{L}/\delta\psi^* = \hat{F}[\psi]$. According to the CVA method, for the trial function $\psi_T[\eta_1, \eta_2, f_i(\xi)]$, we need to solve the following set of extended Euler-Lagrange equations for the variational parameters $f_i(\xi)$ with $i = 1, \ldots, N$

$$\frac{d}{dz}\left(\frac{\partial L}{\partial\left(\frac{\partial f_i}{\partial \xi}\right)}\right) - \frac{\partial L}{\partial f_i} = 2\mathrm{Re}\iint F_{\rm NC}\frac{\partial \psi^*}{\partial f_i} d\eta_1 d\eta_2.$$

Here, L is the average conservative Lagrangian obtained by integration of $\mathcal{L}$ over the transverse coordinates $\eta_{1,2}$.

To solve Eq. (5) we define a Lagrangian density

$$\mathcal{L} = i\left(\psi\frac{\partial \psi^*}{\partial \xi} - \psi^*\frac{\partial \psi}{\partial \xi}\right) - \frac{|\psi|^2}{\alpha^2} + \frac{\ln(1+\alpha^2|\psi|^2)}{\alpha^4} + \sum_{m=\{1,2\}}\left|\frac{\partial \psi}{\partial \eta_m}\right|^2 + g\eta_m^2|\psi|^2, \quad (7)$$

such that $\delta\mathcal{L}/\delta\psi^*$ is the lhs of Eq. (5). We use a trial function in the following form

$$\psi_T(\eta_1, \eta_2, \xi) = A(\xi)\exp\left(i\phi(\xi) + \sum_{m=\{1,2\}} -\frac{[\eta_m - \zeta_m(\xi)]^2}{2a_m^2(\xi)} + ib_m(\xi)\eta_m^2 + ic_m(\xi)\eta_m\right), \quad (8)$$

where $A(\xi)$ is the normalized amplitude of the electric field, $\zeta_{1,2}(\xi)$ defines displacements of a Gaussian along the $\eta_{1,2}$ axes from the origin of the coordinates, $a_{1,2}(\zeta)$ are the normalized widths of the beam in the $\eta_{1,2}$ directions, $b_{1,2}$ are the normalized curvatures of the beam wave front, $c_{1,2}(\zeta)$ are the tilt of inclination of the Gaussian beam along the ξ axis, and $\phi(\zeta)$ is the longitudinal phase; all are real functions of ζ. Here, for simplicity, we don't take into account possible coupling between η_1 and η_2 (term proportional to the product $\eta_1\eta_2$) that could result in orbital angular momentum of elliptical beam as has been shown [47–49].

Using the CVA method for the variables A, $a_{1,2}$, $\zeta_{1,2}$, $b_{1,2}$, $c_{1,2}$, and ϕ in our trial function, we obtain the following set of coupled ordinary differential equations:

$$\frac{dA}{d\xi} = -(b_1 + b_2 + \gamma)A - 3\kappa A^3/4, \quad (9)$$

$$\frac{da_{1,2}}{d\xi} = 2a_{1,2}b_{1,2} + \kappa a_{1,2}A^2/4, \quad (10)$$

$$\frac{d\zeta_{1,2}}{d\xi} = c_{1,2} + 2b_{1,2}\zeta_{1,2}, \quad (11)$$

$$\frac{db_{1,2}}{d\xi} = \frac{1}{2a_{1,2}^4} - 2b_{1,2}^2 - \frac{g}{2} + \frac{\ln(1+\alpha^2A^2) + \mathrm{Li}_2(-\alpha^2A^2)}{2\alpha^4A^2a_{1,2}^2}, \quad (12)$$

$$\frac{dc_{1,2}}{d\xi} = -\frac{\zeta_{1,2}}{2a_{1,2}^4} - 2b_{1,2}c_{1,2} - \frac{\zeta_{1,2}[\ln(1+\alpha^2A^2) + \mathrm{Li}_2(-\alpha^2A^2)]}{\alpha^4A^2a_{1,2}^2}, \quad (13)$$

$$\frac{d\phi}{d\xi} = \frac{1}{2\alpha^2} + \sum_{m=\{1,2\}} \frac{\zeta_m^2 - a_m^2}{2a_m^4} + \frac{\left(\zeta_m^2 - a_m^2\right)\ln(1+\alpha^2A^2)}{2\alpha^4A^2(\xi)a_m^2} - \frac{c_m^2}{2} + \frac{\left(2\zeta_m^2 - a_m^2\right)\mathrm{Li}_2(-\alpha^2A^2)}{4\alpha^4A^2a_m^2}. \quad (14)$$

Here, $\mathrm{Li}_s(x) = \sum_{k=1}^{\infty} \frac{x^k}{k^s}$ is the Spence's or dilogarithm function [50].

For the cubic-quintic model, we change the nonlinear term of Eq. (2) to that of Eq. (3) and using the same CVA technique as before, we again obtain Eqs. (9)–(11) for A, a, and $\zeta_{1,2}$, and new equations for $b_{1,2}$, $c_{1,2}$, and ϕ in the form

$$\frac{db_{1,2}}{d\xi} = \frac{1}{2a_{1,2}^4} - 2b_{1,2}^2 - \frac{g}{2} - \frac{A^2}{a_{1,2}^2}\left[\frac{1}{8} - \frac{QA^2}{9}\right], \quad (15)$$

$$\frac{dc_{1,2}}{d\xi} = -2b_{1,2}c_{1,2} + \frac{\zeta_{1,2}}{a_{1,2}^2}\left[\frac{A^2}{4} - \frac{1}{a_{1,2}^2} - \frac{2QA^4}{9}\right], \quad (16)$$

$$\frac{d\phi}{d\xi} = \left[\frac{3}{8} - \frac{5QA^2}{18}\right]A^2 - \sum_{m=\{1,2\}} \frac{1}{2a_m^2} - \frac{c_m^2}{2} - \frac{\zeta_m^2}{a_m^2}\left[\frac{1}{2a_m^2} - \frac{A^2}{8} + \frac{QA^4}{9}\right]. \quad (17)$$

III. RESULTS AND DISCUSSION

In order to understand the propagation of an elliptic beam in absorbing media, it is necessary to consider first some simpler cases and analyze the behavior of the beam in various propagation regimes as a function of the parameters which characterize the beam shape.

A. Elliptic beam in a lossless medium

Here, we analyze the propagation of an elliptic beam in lossless GRIN waveguides using both saturable and cubic-quintic models for the waveguide material to find the main parameters that define regions of periodic and nonperiodic solutions. For an elliptic beam propagating in a lossless medium where $\gamma = \kappa = 0$, Eqs. (9) and (10) can be simplified to

$$2A(\xi)a_1(\xi)a_2(\xi)\frac{dA}{d\xi} + A^2(\xi)a_2(\xi)\frac{da_1}{d\xi} + A^2(\xi)a_1(\xi)\frac{da_2}{d\xi} = 0. \quad (18)$$

After integration over ζ, we obtain the following solution to Eq. (18)

$$E = A^2(\xi)a_1(\xi)a_2(\xi) = A^2(0)a_1(0)a_2(0), \quad (19)$$

which shows that the energy E is conserved during propagation along the ξ coordinate.

For the saturable model, we combine Eqs. (10), (12), and (19), and obtain the set of coupled ordinary differential equations

$$\frac{d^2u_{1,2}}{d\xi^2} = \frac{1}{a_{1,2}^4(0)u_{1,2}^3} + \frac{u_{2,1}\ln\left(1+\frac{K_{\mathrm{sat}}}{u_1u_2}\right)}{\alpha^2K_{\mathrm{sat}}a_{1,2}^2(0)} + \frac{u_{2,1}\mathrm{Li}_2\left(-\frac{K_{\mathrm{sat}}}{u_1u_2}\right)}{\alpha^2K_{\mathrm{sat}}a_{1,2}^2(0)} - g_{1,2}u_{1,2}, \quad (20)$$

$$\frac{d^2\zeta_{1,2}}{d\xi^2} + g\zeta_{1,2} = 0, \quad (21)$$

where $K_{\mathrm{sat}} = \alpha^2A^2(0)$, $a_{1,2}(\xi) = a_{1,2}(0)u_{1,2}(\xi)$. Integrating Eq. (21) over ξ, we obtain

$$\frac{1}{2}\left(\frac{d\zeta_{1,2}}{d\xi}\right)^2 + \frac{g\zeta_{1,2}^2}{2} = 0, \quad (22)$$

Equation (22) defines the displacement $\zeta_{1,2}(\xi)$ of the unaligned beam relative to the grade index origin. The solution of Eq. (22) gives a sinusoidal dependence of $\zeta_{1,2}(\xi)$ on the frequency $\sqrt{g}$, similar to that for linear media [14,15].

In some cases, the index profile needs to be modified by the addition to Eq. (1) of higher-order terms such as G_1r^4 or G_2r^6 [51]. Analysis of the appropriate equations show that due to higher-order terms, coupling between the breathing and displacement frequencies takes place in both linear and nonlinear media, similar to that reported previously for planar GRIN waveguides [39].

When we integrate Eqs. (20), we find that the beam widths satisfy the dynamical equation for the two-dimensional problem

$$\frac{a_1^2(0)}{2}\left(\frac{du_1}{d\xi}\right)^2 + \frac{a_2^2(0)}{2}\left(\frac{du_2}{d\xi}\right)^2 + \Omega(u_1,u_2) = 0, \quad (23)$$

where

$$\Omega_{\mathrm{sat}}(u_1,u_2) = \frac{\mathrm{Li}_2(-K_{\mathrm{sat}}) - u_1u_2\mathrm{Li}_2\left(-\frac{K_{\mathrm{sat}}}{u_1u_2}\right)}{\alpha^2K_{\mathrm{sat}}} + \sum_{m=\{1,2\}} \frac{1}{2a_m^2(0)}\left(\frac{1}{u_m^2} - 1\right) + \frac{ga_m^2(0)\left(u_m^2-1\right)}{2}. \quad (24)$$

For the cubic-quintic model, we combine Eqs. (10), (15), and (19), and obtain a set of coupled ordinary differential equations similar to Eqs. (20) and (21) with the potential function

$$\Omega_{\mathrm{CQ}}(u_1,u_2) = \frac{QA^4(0)}{9}\left(\frac{1}{u_1^2u_2^2} - 1\right) - \frac{A^4(0)}{4}\left(\frac{1}{u_1u_2} - 1\right) + \sum_{m=\{1,2\}} \frac{1}{2a_m^2(0)}\left(\frac{1}{u_m^2} - 1\right) + \frac{ga_m^2(0)\left(u_m^2-1\right)}{2}. \quad (25)$$

In both models, the behavior of the beam widths $u_{1,2}(\xi)$ during propagation is controlled by the two-dimensional potential function $\Omega(u_1,u_2)$ and can be interpreted as the motion of a "point mass" under the influence of a two-dimensional potential with $\Omega(1,1) = 0$. As was previously shown [36,37], this motion is rather complicated and essentially depends on

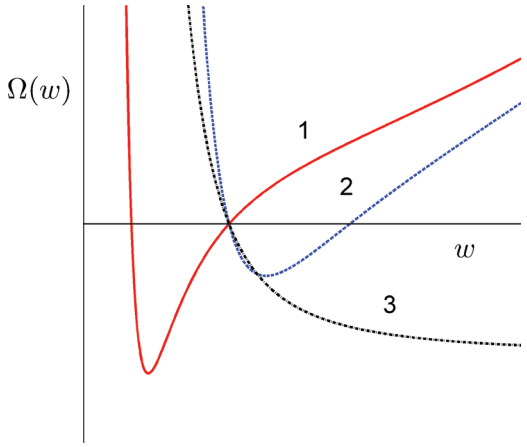

FIG. 1. (Color online) Schematic plots of the potential functions $\Omega(w)$. Curves 1 and 2 correspond to PSF and PSD regimes for GRIN waveguides, respectively. Curve 3 corresponds to diffractive regime in nongraded waveguides but does not exist for GRIN waveguides.

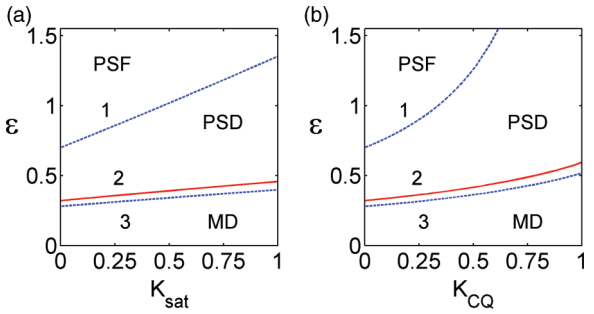

FIG. 2. (Color online) ε, K diagram for GRIN waveguides: (a) saturable model; (b) cubic-quintic model. The curve 1 shows the boundary between PSF and PSD regions for cylindrical beam in GRIN waveguides with $ga_r^4(0) = 0.3$. For an elliptical beam no sharp boundary exists between these regions [36,37]. The MD regime in GRIN waveguides is formally absent both for cylindrical and elliptical beams. At the curves 2 and 3 the final beam widths becomes six times greater than the initial widths for both elliptical and cylindrical beams.

the initial power and geometry of the laser, and the nonlinear properties of the media.

To explain the behavior of the elliptic beam in the GRIN media in a simple way, we write $u_{1,2} = w$ and first consider propagation of a cylindrical Gaussian beam aligned along the fiber axis. In Fig. 1, we plot the potential function $\Omega(w)$ schematically for a GRIN medium in comparison with a nongraded medium. The $\Omega(w)$ is qualitatively similar for both saturable and cubic-quintic media, and also to that of nongraded media [36,37]. The potential defines two different regions of parameter space for the propagation of the beam: periodic self-focusing (PSF) and periodic self-diffracting (PSD). The potential function $\Omega(w)$ has two roots. One of the roots is $w_1 = 1$, and the other root w_2 can be either larger or smaller than 1. The beam width oscillates between w_1 and w_2. When $w_2 < 1$ (curve 1), the beam width oscillates in the PSF regime, whereas when $w_2 > 1$ (curve 2), it oscillates in the PSD regime. For the special case in which $d\Omega(w)/dw|_{w=w_1} = \Omega(w_1) = 0$, the potential well degenerates into a single point, so that a point mass released at this point will remain there. This implies confined beam propagation owing to the exact balance between the competitive forces of self-defocusing and self-focusing. The main difference in $\Omega(w)$ between GRIN media and nongraded media is as follows: the potential function in nongraded media can have either one or two roots, whereas in the GRIN media it has always two roots. This is caused by the asymptotic behavior of $\lim_{w\to\infty}\Omega(w)$ in nongraded media: $\lim_{w\to\infty}\Omega(w)$ tends to a constant value, and depending on the sign of the constant, the beam demonstrates either diffracting behavior [when $\lim_{w\to\infty}\Omega(w) < 0$, see curve 3] or PSF and PSD behavior [when $\lim_{w\to\infty}\Omega(w) > 0$]. In the GRIN media, due to the last (parabolic) term in Eqs. (24) and (25), we have parabolic behavior of $\lim\Omega(w)$, and thus $\Omega(w)$ always has two roots. This means that from a formal point of view, no diffractive regime exists for the GRIN media.

1. ε, K diagrams for GRIN and nongraded media

The behavior of an elliptical beam in a nonlinear medium can be described using ϵ-K diagrams [37–39] where $\varepsilon = A^2(0)a_1(0)a_2(0)/4$ is the beam energy and K is written as $K_{\rm sat} = \alpha A(0)^2$ for the saturable model and $K_{\rm CQ} = QA(0)^2$ for the cubic-quintic model. In Fig. 2, we present diagrams for [Fig. 2(a)] saturable and [Fig. 2(b)] cubic-quintic media, which define various regions of the beam behavior in GRIN waveguides for an elliptical beam in comparison with a cylindrical beam. In the diagrams, $\varepsilon = 1$ corresponds to the critical energy which leads to filamentation of the beam in a Kerr medium ($K_{\rm sat,CQ} = 0$).

For nongraded waveguides, the parameter space is divided into PSF, PSD, and MD regions, as we discussed previously for cubic-quintic [36] and saturable [37] models. The curve 1 shows the boundary between PSF and PSD regimes in GRIN waveguides with $ga_r^4(0) = 0.3$ for cylindrical beam. With the increase of g the curve 1 moves downwards, similarly to our previous calculations for planar waveguides [39]. For an elliptical beam, as was previously shown [36,37], no sharp boundary exists between the PSF and PSD regions. As was shown numerically, the potential function $\Omega(u_1,u_2)$ has a minimum value, which is always negative, and is independent of the values of ε and K. Due to this fact, the elliptical beam widths a_1 and a_2 never reach constant values but oscillate throughout propagation so that it is impossible to completely distinguish between the diffracting and self-focusing oscillatory regions for elliptical beams, as was possible for cylindrical beams.

In the region below the curve 1, the cylindrical beam oscillates in the PSD regime and as ε decreases, the maximum width of the beam increases. Formally, the MD regime is absent in GRIN waveguides. However one can define a line in the diagram that corresponds to a given maximal width. In Fig. 2, the curves 2 and 3 define the lines for the maximal beam widths, which are six times wider than the initial widths for both elliptical and cylindrical beams. The positions of the curves 2 and 3 is very sensitive to g: it moves downwards with increasing g. The curves 2 and 3 in Fig. 2 are shown for $ga_r^4(0) = 0.02$. With the increase in the eccentricity of the ellipse, curve 2 moves up relative to curve 3, which relates to a cylindrical beam.

Along curve 1 the cylindrical beam width stays constant due to the exact balance between the competing forces of diffraction and self-focusing. As one can obtain from Eqs. (24) and (25) with $\eta_{1,2} = w$ (for cylindrical beam), curve 1 for the saturable model is defined by the expression: $4\varepsilon = [-K_{\rm sat}^2 + K_{\rm sat}^2 g a_r^4(0)]/[\ln(1+K_{\rm sat}) + {\rm Li}_2(-K_{\rm sat})]$, whereas for the cubic-quintic model, it is defined by $4\varepsilon = [1 - g a_r^4(0)]/[1/4 - 2K_{\rm CQ}/9]$. When $g = 0$ we obtain the appropriate expressions for nongraded waveguides [36,37].

2. *Breathing and beating periods*

Using numerical methods, we have solved Eqs. (9)–(14) for the saturable model and Eqs. (9)–(13) and (15)–(17) for the cubic-quintic model to find $\eta_{1,2}$ as a function of propagation distance, ξ. To compare the solution with that for cylindrical beam, we defined initial conditions as $A^2(0)a_1(0)a_2(0) = A_r^2(0)a_r^2(0)$, $a_2(0) = \rho a_1(0)$, and $b_{1,2}(0) = c_{1,2}(0) = \phi(0) = 0$. The first condition means that the energies of the cylindrical and elliptical beams are conserved throughout propagation [see Eq. (18)]. Here, $A_r(0)$ and $a_r(0)$ are the amplitude of electric field and the width of the cylindrical beam, and $a_2(0)/a_1(0) = \rho > 1$ is the ratio between the widths of the beam in the $\eta_{1,2}$ directions.

Numerical solution of Eqs. (9)–(17) gives a distance $L_{\rm br}$, which characterizes the oscillations of the beam widths during propagation in either saturable or cubic-quintic media. $L_{\rm br}$ defines a distance between two adjacent minimal (or maximal) width diameters, which vary during propagation along the ξ axis (breathing period). For cylindrical beam in cubic-quintic model the value of $L_{\rm br}$ can be found by solving the appropriate equations analytically (see Appendix).

Previously we showed for nongraded media that in contrast to the cylindrical beam [52–56] whose width oscillates during propagation with constant amplitude, oscillations of both widths a_1 and a_2 occur with periodically varying amplitudes [36,37]. This phenomenon is called "beats". The maximum of a_1 corresponds to the minimum of a_2 and vice versa, due to the condition of energy conservation [see Eq. (18)]. In addition, we found that there are two main types of behavior of the elliptical beam, Type 1 where the orientation of the ellipse does not change on propagation, and Type 2 where the major and minor axes interchange during propagation. We found that the type of beats in the saturable model depends on the ε and K of Fig. 2 and at low ε is not very sensitive to the ellipticity ρ. For the cubic-quintic model, the beating type is controlled not only by ε and K but also by the ellipticity of the incident beam, and is extremely sensitive to small changes in ρ.

Here, we extend this approach to GRIN media and calculate both breathing ($L_{\rm br}$) and beating ($L_{\rm beat}$) periods for various ellipticities ρ at some specific (ε, K) points on the diagram shown in Fig. 2. The dependence of the ratio $L_{\rm beat}/L_{\rm br}$ on the parameter ρ for both saturable and cubic-quintic models is presented in Fig. 3 for the case where the beating is initially of Type 2.

We see, for the saturable model [Fig. 3(a)], that the ratio increases slightly with increasing g and decreases monotonically with ρ; the same behavior is obtained for Type 1. In addition, it can be shown that the beating type remains constant throughout. In contrast, for the cubic-quintic model, we see in Fig. 3(b) that the ratio $L_{\rm beat}/L_{\rm br}$ varies nonmonotonically with ρ and displays singularities. It can be shown that these singularities are accompanied by transitions between different beating types: Type 2 transfers to Type 1 and then reverts to Type 2. These singularities move to larger values of ρ with increasing GRIN index g. It should be noted that the same general behavior is obtained for different values of (ε, K). In addition, the curves remain unchanged provided the values of ε, K and $g a_1^2(0)a_2^2(0)$ are kept constant.

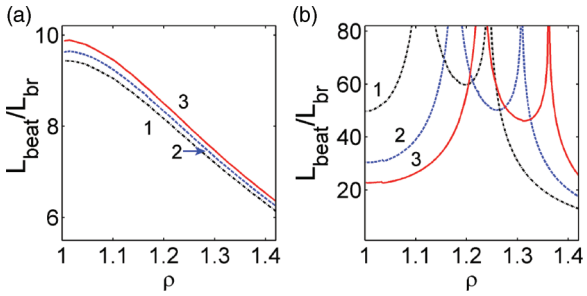

FIG. 3. (Color online) Typical dependencies of the ratio $L_{\rm beat}/L_{\rm br}$ on the parameter ρ for (a) saturable and (b) cubic-quintic models, which are characterized by various values of the GRIN index g. Curve 1 relates to $g a_1^2(0)a_2^2(0) = 0$, curve 2 to $g a_1^2(0)a_2^2(0) = 0.01$, and curve 3 to $g a_1^2(0)a_2^2(0) = 0.02$. The plots correspond to $(\varepsilon, K) = (2.822, 0.682)$ for the saturable model and $(\varepsilon, K) = (2.039, 0.682)$ for the cubic-quintic model.

Type 1 and Type 2 behavior of a beam as it propagates through the lossless medium can be seen in the movies [59].

B. Elliptic beam in a lossy medium

Using Eqs. (9)–(17) we can describe the propagation of elliptical Gaussian beam in both saturable and cubic-quintic GRIN waveguides, taking into account linear and nonlinear absorption, which are characterized by the values of γ and κ. A potential well in the lossy media cannot be defined and the regions for the motion of a point mass cannot be separated as was done in Fig. 2 for lossless media. However, it is clear that due to the energy dissipation during the propagation, the beam has to cross the oscillatory region PSF towards the PSD region of the (ε, K) parameter space.

In Fig. 4, we show the propagation of an elliptical beam in an absorbing medium. It is qualitatively similar for both the saturable and cubic-quintic models. In Fig. 4(a), we compare the oscillations of the beam width $a_1(\xi)$ for GRIN and nongraded media, whereas in Fig. 4(b) we show typical oscillations of $a_{1,2}(\xi)$ in a GRIN medium. The propagation begins from the PSF region of Fig. 2 where beats exist. After some propagation distance, the beam widths $a_{1,2}(\xi)$ in the nongraded media increases monotonically with ξ, whereas in the GRIN medium the oscillations of the beam widths $a_{1,2}(\xi)$ are stabilized. When the beam energy becomes low enough, so that one can neglect nonlinear processes, the CVA method gives the following formula for the beam widths:

$$a_{1,2}(\xi) \propto a_{1,2}(0)\sqrt{\cos^2(\sqrt{g}\xi) + \sin^2(\sqrt{g}\xi)/\left[a_{1,2}^4(0)g\right]}. \tag{26}$$

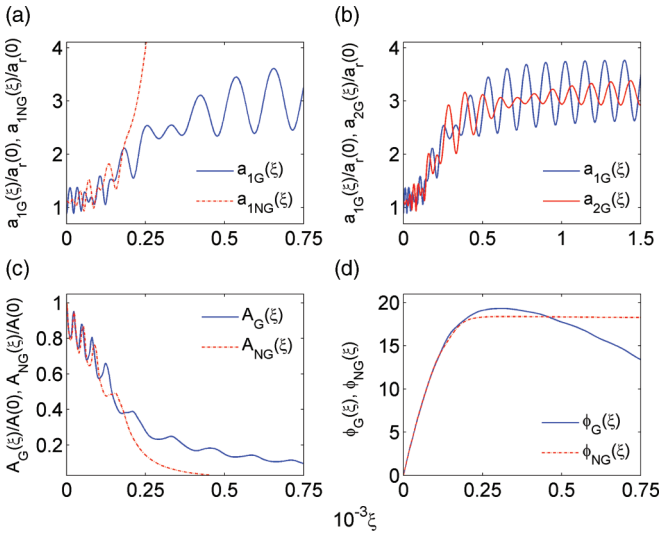

FIG. 4. (Color online) Variation of the beam widths (a) and (b), amplitudes of electric field (c), and phases (d) in GRIN waveguides in absorbing cubic-quintic media in comparison with nongraded waveguides.

As one can see, the width oscillates with amplitude and frequency that depend on g and the initial widths $a_{1,2}(0)$.

The variations of the amplitude of the electric field $A(\xi)$ and the phase $\phi(\xi)$ are presented in Figs. 4(c) and 4(d) for GRIN and nongraded media. With the decrease of the beam energy $\varepsilon(\xi)$, the amplitude of the oscillations of $A(\xi)$ decreases monotonously in both GRIN and nongraded media; in the GRIN media this occurs more slowly than in the nongraded one. The amplitude $A(\xi)$ decreases exponentially according to the expression

$$A(\xi) \propto A(0)\sqrt{g}e^{-\gamma\xi} \times \prod_{m=1,2} a_m(0) \Big/ \sqrt[4]{a_m^4(0)g\cos^2(\sqrt{g}\xi) + \sin^2(\sqrt{g}\xi)}. \tag{27}$$

The phase [Fig. 4(d)] approaches a constant value asymptotically for the case of a nongraded medium. However, for a GRIN medium, the phase decreases linearly and at some propagation distance becomes negative, similar to that reported previously for planar GRIN waveguides [39].

IV. CONCLUSION

We have analyzed the propagation of elliptical Gaussian beam in GRIN waveguides with parabolic index profile for both cubic-quintic and saturable models of a nonlinear media, and compared the results with those for nongraded waveguides. We constructed diagrams, which define regions of self-focusing and self-diffractive beam propagation for both types of media in the absence of loss. We found that propagating pulses exhibit an oscillatory pattern, similar to the breathing and beating behavior in nongraded waveguides [36,37]. We distinguished beats of Type 1 for which the orientation of the ellipse does not change on propagation, and beats of Type 2 where the major and minor axes interchange during propagation. We calculated the dependence of the ratios of breathing and beating frequency oscillations $L_{\rm beat}/L_{\rm br}$ on the beam ellipticity ρ, and the GRIN index g. We have found a marked difference in the dependence of $L_{\rm beat}/L_{\rm br}$ on ρ between the saturable and cubic-quintic media: in the saturable model, $L_{\rm beat}/L_{\rm br}$ is a monotonic function of ρ, whereas in the cubic-quintic model, the dependence of $L_{\rm beat}/L_{\rm br}$ on ρ is characterized by singularities, which correspond to transitions between the two types of beat oscillations. The positions of these singularities move to higher ellipticity with increasing values of the GRIN index. We have also investigated breathing and beating of an elliptical Gaussian beam, taking into account both linear and nonlinear absorption. We have calculated the variation of the beam widths, amplitudes and phases, as functions of the propagation distance and demonstrated the differences between the breathing behavior in GRIN and nongraded waveguides. If the spatial profile of the beam and the center of the index profile are not aligned, the pulse oscillates around the index origin at a displacement frequency proportional to $\sqrt{g}$, similar to the behavior found in linear media [14,15].

APPENDIX: ANALYTICAL SOLUTION FOR CYLINDRICAL GAUSSIAN BEAM IN CUBIC-QUINTIC GRIN MODEL

For a GRIN cubic-quintic medium interacting with a cylindrical Gaussian beam, in which $a_{1,2}(0) = a_r(0)$ and $u_{1,2}(\xi) = w(\xi)$, one can find an analytical solution of the dynamical equation, which can be written in the form

$$\frac{1}{2}\left(\frac{dw}{d\xi}\right)^2 + \Omega_{\rm CQ}(w) = 0, \tag{A1}$$

where

$$\Omega_{\rm CQ}(w) = \frac{\mu_r}{w^2(\xi)} - \frac{\nu_r}{w^2(\xi)} + \frac{\lambda_r}{w^4(\xi)} + \frac{gw^2(\xi)}{2} - \left(\mu_r - \nu_r + \lambda_r + \frac{g}{2}\right), \tag{A2}$$

with

$$\mu_r = \frac{1}{2a_r^4(0)}, \quad \nu_r = \frac{A(0)^2}{8a_r^2(0)}, \quad \lambda_r = \frac{QA(0)^4}{18a_r^2(0)}.$$

It can be shown that the potential function $\Omega_{\rm CQ}(w)$ has two real roots: $w_1 = 1$, and $w_2 = \sqrt{[\mu_r - \nu_r + \lambda_r + \sqrt{(\mu_r - \nu_r + \lambda_r)^2 + 2\lambda_r g}]/g}$. The analytical solution of Eq. (A1) can be written as follows: For $2(\nu_r - \mu_r - 2\lambda_r) + g < 0$ (PSD regime),

$$\xi = \frac{\Pi\left(\sqrt{\frac{d_1(w^2-1)}{w^2(d_1-1)}}, \frac{d_1-1}{d_1}, \sqrt{\frac{d_1d_2-d_2}{d_1d_2+d_1}}\right)}{\sqrt{(d_1+d_1d_2)g}}. \tag{A3}$$

For $2(\nu_r - \mu_r - 2\lambda_r) + g > 0$ (PFD regime),

$$\xi = \frac{(d_2+1)\Pi\left(\sqrt{\frac{(d_1+d_2)(1-w^2)}{(1-d_1)(d_2+w^2)}}, \frac{d_1-1}{d_1+d_2}, \sqrt{\frac{d_2-d_1d_2}{d_1+d_2}}\right)}{\sqrt{(d_1+d_2)g}} - \frac{d_2F\left(\sqrt{\frac{(d_1+d_2)(1-w^2)}{(1-d_1)(d_2+w^2)}}, \sqrt{\frac{d_2-d_1d_2}{d_1+d_2}}\right)}{\sqrt{(d_1+d_2)g}}. \tag{A4}$$

Here, $d_{1,2}=[\pm(\mu_r-\nu_r+\lambda_r)+\sqrt{(\mu_r-\nu_r+\lambda_r)^2+2\lambda_r g}]/g$; F,K,Π are the incomplete and complete elliptic integrals of the first, second, and third kinds, respectively [57].

The distance L equals 2ξ when $w\to w_2$, so that

$$L=\frac{2\Pi\left(\frac{d_1-1}{d_1},\sqrt{\frac{d_1d_2-d_2}{d_1d_2+d_1}}\right)}{\sqrt{(d_1+d_1d_2)g}}\quad\text{PSD regime,}\tag{A5}$$

and

$$L=\frac{2(d_2+1)\Pi\left(\frac{d_1-1}{d_1+d_2},\sqrt{\frac{d_2-d_1d_2}{d_1+d_2}}\right)}{\sqrt{(d_1+d_2)g}}-\frac{2d_2K\left(\sqrt{\frac{d_2-d_1d_2}{d_1+d_2}}\right)}{\sqrt{(d_1+d_2)g}}\quad\text{PSF regime.}\tag{A6}$$

It is easy to show from Eq. (A6) that in the nongraded medium, for which the boundary between PSD and diffractive regions is defined as $\nu_r=\mu_r+\lambda_r$, the distance L can be expressed in the form

$$L=\frac{\sqrt[4]{8}\Pi\left(1-\sqrt{\frac{g}{2\lambda_r}},\frac{\sqrt{2\lambda_r-g}}{\sqrt{2\lambda_r}+\sqrt{g}}\right)}{\sqrt{\sqrt{2}\lambda_r+\sqrt{g\lambda_r}}},\tag{A7}$$

so that when $g\to 0$, $L\to\infty$ as in a diffractive regime.

Moreover, substituting $g\to 0$ in Eqs. (A3)–(A6), one obtains an analytical solution identical to that previously reported for a nongraded cubic-quintic medium [52–56], whereas substituting $\nu_r,\lambda_r\to 0$ in Eqs. (A3)–(A6), we obtain the analytical solution for a linear medium [14,15,27]: $w=\sqrt{\cos^2(\sqrt{g}\xi)+\sin^2(\sqrt{g}\xi)/[a_r^4(0)g]}$.

Recently, an analytical solution for the breathing period was obtained for Kerr GRIN media [48,58] using the Ermakov-Ray-Reid reduction method. These results can easily be obtained from our Eqs. (A5) and (A6) by substituting the quintic variable $\lambda_r=0$.

[1] Y. S. Kivshar and G. P. Agrawal, *Optical Solitons* (Academic Press, New York, 2003).
[2] G. P. Agrawal, *Nonlinear Fiber Optics* (Academic Press, New York, 2007).
[3] N. Akhmediev and A. Ankkiewicz, *Dissipative Solitons* (Springer, Berlin, 2005).
[4] K. Iga, Y. Kokubun, and M. Oikawa, *Fundamentals of Microoptics: Distributed-Index, Microlens, and Stacked Planar Optics* (Academic Press, Tokyo, 1981).
[5] S. Sinzinger and J. Jahns, *Microoptics*, 2nd ed. (Wiley VCH, New York, 2003).
[6] M. D. Pelusi, V. G. Taeed, L. Fu, E. Magi, M. R. E. Lamont, S. Madden, D.-Y. Choi, D. A. P. Bulla, B. Luther-Davies, and B. J. Eggleton, IEEE J. Sel. Top. Quantum Electron **14**, 529 (2008).
[7] M. H. Frosz, A. Stefani, and O. Bang, Opt. Express **19**, 10471 (2011).
[8] B. Gu, W. Yuan, M. H. Frosz, A. Ping-Zhang, S. He, and O. Bang, Opt. Lett. **37**, 794 (2012).
[9] J. Hu, M. Torregiani, F. Morichetti, N. Carlie, A. Agarwal, K. Richardson, L. C. Kimerling, and A. Melloni, Opt. Lett. **35**, 874 (2010).
[10] R. W. Boyd, *Nonlinear Optic*, 3rd ed. (Elsevier, Amsterdam, 2008).
[11] Y. H. Kim, B. H. Lee, Y. Chung, U. C. Paek, and W. T. Han, Opt. Lett. **27**, 580 (2002).
[12] S. Moon, A. Lin, B. H. Kim, P. R.Watekar, and W. T. Han, J. Non-Cryst. Solids **354**, 602 (2008).
[13] S. Ju, P. R. Watekar, and W. T. Han, Opt. Express **19**, 2599 (2011).
[14] M. S. Sodha and A. K. Ghatak, *Inhomogeneous Optical Waveguides* (Plenum Press, New York, 1977).
[15] A. K. Ghatak and K. Thyagarajan, *Contemporary Optics* (Plenum Press, New York, 1978).
[16] S. Longhi and D. Janner, J. Opt. B: Quantum Semiclassical **6**, S303 (2004).
[17] J. T. Manassah, P. L. Baldeck, and R. R. Alfano, Opt. Lett. **13**, 589 (1988).
[18] L. Gagnon and C. Pare, J. Opt. Soc. Am. A **8**, 601 (1991).
[19] A. M. Goncharenko, Y. A. Logvin, A. M. Samson, and P. S. Shapovalov, Opt. Commun. **81**, 225 (1999).
[20] M. Karlsson, D. Anderson, and M. Desaix, Opt. Lett. **17**, 22 (1992).
[21] J. T. Manassah, Opt. Lett. **17**, 1259 (1992).
[22] D. Anderson and M. Lisak, Phys. Scr., T **63**, 69 (1996).
[23] Z. Jovanoski, Phys. Scr. **59**, 446 (1999).
[24] Y. Li, J. Opt. Soc. Am. B **17**, 555 (2000).
[25] P. Berczynski, Y. Kravtsov, and G. Zeglinski, Cent. Eur. J. Phys **6**, 603 (2008).
[26] P. Berczynski, J. Opt. **13**, 035707 (2011).
[27] C. Gomez-Reino, Int. J. Optoelectron. **7**, 607 (1992).
[28] V. P. Kandidov and V. Y. Fedorov, Quantum Electron. **34**, 1163 (2004).
[29] O. Bang, W. Krolikowski, J. Wyller, and J. J. Rasmussen, Phys. Rev. E **66**, 046619 (2002).
[30] O. Bang, D. Edmundson, and W. Krolikowski, Phys. Rev. L **83**, 5479 (1999).
[31] O. Bang, P. L. Christiansen, F. If, K. O. Rasmussen, and Y. B. Gaididei, Phys. Rev. E **49**, 4627 (1994).
[32] O. Bang, J. J. Rasmussen, and P. L. Christiansen, Nonlinearity **7**, 205 (1994).
[33] J. J. Rasmussen and K. Rypdal, Phys. Scr. **33**, 481 (1986).
[34] F. Dalfovo, S. Giorgini, L. Pitaevskii, and S. Stringari, Rev. Mod. Phys **73**, 463 (1999).
[35] F. K. Abdullaev, A. Gammal, L. Tomio, and T. Frederico, Phys. Rev. A **63**, 043604 (2001).
[36] D. Ianetz, Y. Kaganovskii, A. D. Wilson-Gordon, and M. Rosenbluh, Phys. Rev. A **81**, 053851 (2010).
[37] D. Ianetz, Y. Kaganovskii, A. D. Wilson-Gordon, and M. Rosenbluh, Phys. Rev. A **82**, 065803 (2010).
[38] D. Ianetz, Y. Kaganovskii, A. D. Wilson-Gordon, and M. Rosenbluh, Opt. Commun. **284**, 5212 (2011).

[39] D. Ianetz, Y. Kaganovskii, and A. D. Wilson-Gordon, Opt. Commun. **285**, 3636 (2012).
[40] Y. F. Chen, K. Beckwitt, F. W. Wise, and B. A. Malomed, Phys. Rev. E **70**, 046610 (2004).
[41] D. Anderson, Phys. Rev. A **27**, 3135 (1983).
[42] B. A. Malomed, Prog. Opt. **43**, 71 (2002).
[43] M. Bonnedal, D. Anderson, and M. Lisak, Phys. Scr. **20**, 479 (1979).
[44] J. G. Caputo, N. Flytzanis, and M. P. Sørensen, J. Opt. Soc. Am. B **12**, 139 (1995).
[45] S. Chavez Cerda, S. B. Cavalcanti, and J. M. Hickmann, Eur. Phys. J. D **1**, 313 (1998).
[46] A. Scott, *Encyclopedia of Nonlinear Science* (Routledge, New York, 2005).
[47] A. S. Desyatnikov, D. Buccoliero, M. R. Dennis, and Y. S. Kivshar, Phys. Rev. Lett. **104**, 053902 (2010).
[48] J. Abdullaev, A. S. Desyatnikov, and E. A. Ostrovskaya, J. Opt. **13**, 064023 (2011).
[49] A. S. Desyatnikov, M. R. D. D. Buccoliero, and Y. S. Kivshar, Sci. Rep **2**, 00771 (2012).
[50] M. Abramowitz and I. A. Stegun, *Handbook of Mathematical Functions* (Dover, New York, 1970).
[51] M. J. Adams, *An Introduction to Optical Waveguides* (Wiley, New York, 1981).
[52] D. Anderson and M. Bonnedal, Phys. Fluids **22**, 105 (1979).
[53] Z. Jovanoski and R. A. Sammut, J. Nonlinear Opt. Phys. Mater. **6**, 209 (1997).
[54] Z. Jovanoski and R. A. Sammut, Phys. Scr. **57**, 233 (1998).
[55] D. S. Freitas, J. R. D. Oliveira, and M. A. D. Mourao, J. Phys. A **31**, 1761 (1998).
[56] M. Karlsson, Phys. Rev. A **46**, 2726 (1992).
[57] P. F. Byrd and M. D. Friedman, *Handbook of Elliptic Integrals for Engineers and Scientists* (Springer-Verlag, New York, 1971).
[58] C. Rogers, B. Malomed, and H. An, Stud. Appl. Math **129**, 389 (2012).
[59] See Supplemental Material at http://link.aps.org/supplemental/10.1103/PhysRevA.87.043839 for illustration of elliptical beam profile on propagation in a lossless medium.